Inorganic Chemistry

ARTICLE

pubs.acs.org/IC

Synthesis, Structures, and Magnetic Behavior of a Series of Copper(II) Azide Polymers of Cu_4 Building Clusters and Isolation of a New Hemiaminal Ether as the Metal Complex

Sandip Mukherjee,[†] Bappaditya Gole,[†] You Song,[‡] and Partha Sarathi Mukherjee*[,†]

[†]Department of Inorganic and Physical Chemistry, Indian Institute of Science, Bangalore 560012, India

[‡]State Key Laboratory of Coordination Chemistry, Nanjing University, Nanjing 210093, China

Supporting Information

ABSTRACT: Four new neutral copper azido polymers, $[Cu_4(N_3)_8(L^1)_2]_n$ (**1**), $[Cu_4(N_3)_8(L^2)_2]_n$ (**2**), $[Cu_4(N_3)_8(L^3)_2]_n$ (**3**), and $[Cu_9(N_3)_{18}(L^4)_4]_n$ (**4**) [L^{1-4} are formed in situ by reacting pyridine-2-carboxaldehyde with 2-[2-(methylamino)ethyl]pyridine (mapy, L^1), *N*,*N*-dimethylethylenediamine (*N*,*N*-dmen, L^2), *N*,*N*-diethylethylenediamine (*N*,*N*-deen, L^3), and *N*,*N*,2,2-tetramethylpropanediamine (*N*,*N*,2,2-tmpn, L^4)], have been synthesized by using 0.5 mol equiv of the chelating tridentate ligands with $Cu(NO_3)_2 \cdot 3H_2O$ and an excess of NaN_3. Single-crystal X-ray structures show that the basic unit of these complexes, especially **1**−**3**, contains very similar Cu^{II}_4 building blocks. The overall structure of **3** is two-dimensional, while the other three complexes are one-dimensional in nature. Complex **1** represents a unique example containing hemiaminal ether arrested by copper(II). Complexes **1** and **2** have a rare bridging azido pathway: both end-on and end-to-end bridging azides between a pair of Cu^{II} centers. Cryomagnetic susceptibility measurements over a wide range of temperature exhibit dominant ferromagnetic behavior in all four complexes. Density functional theory calculations (B3LYP functional) have been performed on complexes **1**−**3** to provide a qualitative theoretical interpretation of their overall ferromagnetic behavior.

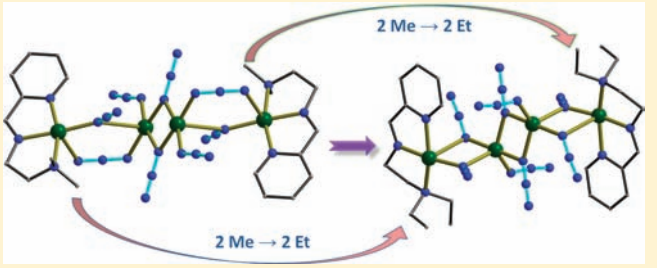

INTRODUCTION

The design and synthesis of multidimensional coordination polymers has attracted unabated attention during the last 2 decades, motivated not only by their structural and topological novelty but also by the potential practical applications of these materials in fields such as molecular magnetism, electrical conductivity, catalysis, molecular absorption, ion exchange, etc.[1]

Despite interest in the properties of such complexes, synthetic methods have yet to achieve the level of competence attained with mononuclear complexes. Molecular magnetic materials are usually constructed through a building-block approach (designed assembly) or by serendipitous assembly, combining paramagnetic transition- or lanthanide-metal ions with suitable bridging ligands that allow for magnetic exchange coupling. The nature of the exchange coupling (sign and magnitude) depends mainly on the bridging ligand (bridging mode and geometry). Only a small number of polyatomic bridging ligands (cyanide, oxalate, dicyanamide, azide, pyrimidine, imidazole, carboxylate, etc.) have been shown to be capable of mediating strong magnetic coupling between transition-metal ions, which, in some cases, leads to bulk magnetic ordering.[2]

The density functional theory (DFT) study of exchange interactions between paramagnetic metal centers through various bridging ligands has also proved to be very fruitful for understanding the fundamental factors governing the magnetic properties of transition-metal compounds.[3]

Metal azido systems with various structures have been widely studied because of the enormous number of opportunities available with this versatile pseudohalide for the building of higher-dimensional complexes as well as its well-known adjustable exchange properties. The end-on (EO) bridging mode generally results in a predictable exchange coupling depending mainly on the bridging angle, while the end-to-end (EE) mode mediates antiferromagnetic interaction with very few exceptions.[4−10]

With a large number of bridging modes, an azido anion provides great opportunities for the building of higher-dimensional materials with intriguing magnetic properties. However, auxiliary blocking ligands also can play a vital role when used prudently. We have recently shown the effect of the relative molar quantities of copper and the diamine ligand on the structure and magnetic properties of the neutral copper azido systems.[10] The use of lower equivalents of blocking amine is expected to increase the coordination sites available around the metal center, which, in turn, allows a short bridging ligand like azide to bring several metal ions closer and prefers the formation of clusters as building units. Here we report our studies on the use of tridentate blocking ligands, derived from simple condensation

Received: December 29, 2010
Published: March 17, 2011

Scheme 1. Four Tridentate Ligands Used in the Present Study

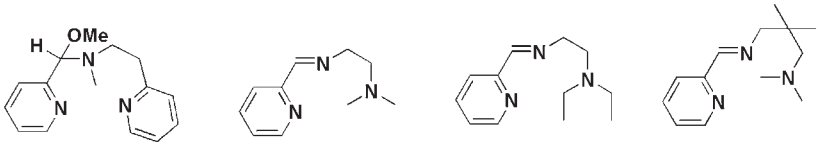

L^1 L^2 L^3 L^4

Table 1. Crystallographic Data and Refinement Parameters for 1−4

	1	2	3	4
empirical formula	$C_{30}H_{38}N_{30}O_2Cu_4$	$C_{20}H_{30}N_{30}Cu_4$	$C_{24}H_{38}N_{30}Cu_4$	$C_{52}H_{84}N_{66}Cu_9$
fw	1105.01	944.90	1000.94	2205.58
T (K)	293(2)	293(2)	293(2)	293(2)
cryst syst	triclinic	monoclinic	monoclinic	triclinic
space group	$P\bar{1}$	$P2_1/n$	$P2_1/n$	$P\bar{1}$
a (Å)	9.9271(16)	8.7634(14)	11.0755(10)	10.9200(3)
b (Å)	10.6663(18)	17.151(3)	11.1386(8)	11.1292(3)
c (Å)	11.4566(19)	12.1511(19)	16.5852(14)	20.3016(5)
α (deg)	106.620(3)	90.00	90.00	91.627(1)
β (deg)	108.265(3)	90.496(11)	103.199(4)	90.081(1)
γ (deg)	90.265(3)	90.00	90.00	115.390(1)
V (Å^3)	1097.9(3)	1826.3(5)	1992.0(3)	2227.81(10)
Z	2	4	4	1
ρ_{calcd} (g cm^{-3})	1.671	1.718	1.669	1.644
μ(Mo Kα) (mm^{-1})	1.980	2.361	2.169	2.180
λ (Å)	0.710 73	0.710 73	0.710 73	0.710 73
F(000)	560.0	952.0	1016	1119
collected reflns	12 673	13 851	34 974	47 173
unique reflns	5101	5422	6045	13 405
GOF (F^2)	1.028	1.015	1.007	0.996
R_1[a]	0.0599	0.0678	0.0477	0.0444
wR_2[b]	0.1332	0.1258	0.0921	0.0870

[a] $R_1 = \Sigma||F_o| - |F_c||/\Sigma|F_o|$. [b] $wR_2 = [\Sigma\{w(F_o^2 - F_c^2)^2\}/\Sigma\{w(F_o^2)^2\}]^{1/2}$.

reactions of pyridine-2-carboxaldehyde and four different diamines.

The synthesis and structures, including the magnetic properties of $[Cu_4(N_3)_8(L^1)_2]_n$ (**1**), $[Cu_4(N_3)_8(L^2)_2]_n$ (**2**), $[Cu_4(N_3)_8(L^3)_2]_n$ (**3**), and $[Cu_9(N_3)_{18}(L^4)_4]_n$ (**4**) [Scheme 1; L^{1-4} are formed in situ by reacting pyridine-2-carboxaldehyde with 2- [2-(methylamino)-ethyl]pyridine (mapy, L^1), *N*,*N*-dimethylethylenediamine (*N*,*N*-dmen, L^2), *N*,*N*-diethylethylenediamine (*N*,*N*-deen, L^3), and *N*,*N*,2,2-tetramethylpropanediamine (*N*,*N*,2,2-tmpn, L^4)], are presented, along with the theoretical treatment of **1**−**3** through DFT studies. Hemiaminal ethers are well-known unstable intermediates and spontaneously transform to enamines or dissociate into reactants immediately upon formation. Complex **1** in the present paper represents a unique example where a new hemiaminal ether has been isolated in metal-arrested form. Between **2** and **3**, a dramatic structural change is observed just through an exchange of the two methyl groups in L^2 by two ethyl groups in L^3. Moreover, in **1** and **2**, the peripheral metal atoms are bridged simultaneously by EO and EE azido groups, which is very rare. This unusual bonding mode, in turn, carries the Cu−N_{EO}−Cu angle beyond 130° in both complexes, and to the best of our knowledge, the angle in **2** is the largest (134.7°) observed so far.

EXPERIMENTAL SECTION

Materials. $Cu(NO_3)_2\cdot 3H_2O$, NaN_3, pyridine-2-carboxaldehyde, 2--[2-(methylamino)ethyl]pyridine (mapy), *N*,*N*-dimethylethylenediamine (*N*,*N*-dmen), *N*,*N*-diethylethylenediamine (*N*,*N*-deen), and *N*,*N*,2,2-tetramethylpropanediamine (*N*,*N*,2,2-tmpn) were obtained from commercial sources and were used as received without further purification.

Physical Measurements. Elemental analyses of C, H, and N were performed using a Perkin-Elmer 240C elemental analyzer. IR spectra were recorded as KBr pellets using a Magna 750 FT-IR spectrophotometer. The powder X-ray diffraction (XRD) data were collected using a D8 Advance X-ray diffractometer to verify the phase purity of these complexes (Figure S1 in the Supporting Information). The measurements of variable-temperature magnetic susceptibility were carried out on a Quantum Design MPMS-XL5 SQUID magnetometer. Susceptibility data were collected using an external magnetic field of 0.2 T for all complexes in the temperature range of 1.8−300 K. The experimental susceptibility data were corrected for diamagnetism (Pascal's tables).[11] Magnetizations of all complexes were also measured in the field ranging from −7 to +7 T at 1.8 K, but no hysteresis loop was observed (Figure S6 in the Supporting Information).

Caution! *Although we did not experience any problems with the compounds reported in this work, azido complexes of metal ions in the*

dx.doi.org/10.1021/ic102580a |*Inorg. Chem.* 2011, 50, 3621–3631

Table 2. Selected Bond Distances (Å) and Angles (deg) for 1 and 2 in a 1/2 Format[a]

Cu1−N1	1.978(4)/2.029(4)	Cu1−N2	2.097(4)/1.961(4)
Cu1−N3	1.973(4)/2.068(4)	Cu1−N4	2.018(4)/1.962(4)
Cu1−N6$^{\#1/\#3}$	2.899(5)/2.645(5)	Cu1−N7	2.579(5)/2.645(5)
Cu2−N4	2.689(4)/2.641(4)	Cu2−N9	1.983(4)/1.973(4)
Cu2−N10	1.915(5)/1.930(5)	Cu2−N13	2.005(4)/2.012(4)
Cu2−N13$^{\#2/\#4}$	1.972(4)/2.020(4)	C6−N2	1.489(6)/1.256(6)
N1−Cu1−N2	81.61(2)/80.35(2)	N2−Cu1−N3	91.84(2)/83.39(2)
Cu1−N4−Cu2	131.09(2)/134.71(2)	Cu2−N13−Cu2$^{\#2/\#4}$	103.41(2)/103.28(2)

[a] Symmetry transformations used to generate equivalent atoms: #1, $-x$, $-y+1$,$-z$; #2, $-x-1$, $-y+1$, $-z$; #3, $-x+2$, $-y$, $-z+1$; #4, $-x+1$, $-y$, $-z+1$.

Table 3. Selected Bond Distances (Å) and Angles (deg) for 3 and 4[a]

3					
Cu1−N1	2.098(3)	Cu1−N2	1.951(2)	Cu1−N3	2.123(2)
Cu1−N4	1.959(2)	Cu1−N7	2.610(5)	Cu1−N9$^{\#5}$	2.383(3)
Cu2−N4	2.208(2)	Cu2−N7	2.000(3)	Cu2−N10	1.975(4)
Cu2−N13	1.992(3)	Cu2−N13$^{\#6}$	2.128(3)	C6−N2	1.263(4)
N1−Cu1−N2	78.92(10)	N2−Cu1−N3	83.46(10)		
Cu1−N4−Cu2	108.60(11)	Cu1−N7−Cu2	93.60(11)		
Cu2−N13−Cu2$^{\#6}$	101.29(12)				
4					
Cu1−N1	1.990(2)	Cu1−N1$^{\#7}$	1.990(2)	Cu1−N4	1.999(2)
Cu1−N4$^{\#7}$	1.999(2)	Cu1−N19	2.591(2)	Cu2−N1	1.977(2)
Cu2−N4	2.022(2)	Cu2−N7	2.014(2)	Cu2−N10	1.974(2)
Cu2−N22$^{\#8}$	2.263(2)	Cu3−N7	2.015(2)	Cu3−N10	2.006(2)
Cu3−N13	1.953(3)	Cu3−N16	1.958(3)	Cu3−N25	2.663(2)
Cu4−N19	1.989(2)	Cu4−N22	2.242(2)	Cu4−N28	2.038(2)
Cu4−N29	2.010(2)	Cu4−N30	2.070(2)	Cu5−N24	2.447(3)
Cu5−N25	1.987(2)	Cu5−N27$^{\#9}$	2.729(3)	Cu5−N31	2.042(2)
Cu5−N32	2.012(2)	Cu5−N33	2.059(2)		
Cu1−N1−Cu2	101.63(10)	Cu1−N4−Cu2	99.78(10)		
Cu2−N7−Cu3	101.09(12)	Cu2−N10−Cu3	102.85(12)		

[a] Symmetry transformations used to generate equivalent atoms: #5, $-x+{}^{3}/_{2}$, $y+{}^{1}/_{2}$, $-z+{}^{1}/_{2}$; #6, $-x+2$, $-y$, $-z+1$; #7, $-x+1$, $-y+2$, $-z$; #8, $x+1$, y, z; #9, $-x+1$, $-y+2$, $-z+1$.

presence of organic ligands are potentially explosive. Only a small amount of the material should be prepared, and it should be handled with care.

*Synthesis of the Complex $[Cu_4(N_3)_8(L^1)_2]_n$ (**1**).* A 5 mL methanolic solution of pyridine-2-aldehyde (1 mmol, 107 mg) and mapy (1 mmol, 136 mg) was refluxed for 15 min and was added slowly (hot) to a hot methanolic solution (10 mL) of $Cu(NO_3)_2\cdot 3H_2O$ (2 mmol, 484 mg). After this mixture was stirred and heated at 50 °C for 5 min, a hot aqueous solution (5 mL) of NaN_3 (20 mmol, 1300 mg) was added slowly. The mixture was stirred for 15 min (at 50 °C) and filtered. Rectangular black crystals of **1** were obtained in 12 h from the filtrate. Isolated yield: 60%. Anal. Calcd for **1**, $C_{30}H_{38}N_{30}O_2Cu_4$: C, 32.61; H, 3.47; N, 38.03. Found: C, 32.74; H, 3.44; N, 38.01. IR (KBr, cm^{-1}): 2029, 2049, and 2071 for the azido groups.

*Synthesis of the Complex $[Cu_4(N_3)_8(L^2)_2]_n$ (**2**).* A 5 mL methanolic solution of pyridine-2-aldehyde (1 mmol, 107 mg) and *N*,*N*-dmen (1 mmol, 88 mg) was refluxed for 15 min, and after cooling to room temperature, it was added slowly to a methanolic solution (10 mL) of $Cu(NO_3)_2\cdot 3H_2O$ (2 mmol, 484 mg). After this mixture was stirred for 5 min, an aqueous solution of NaN_3 (20 mmol, 1300 mg) dissolved in 5 mL of water was added slowly. The mixture was stirred for 15 min and filtered. Rectangular black crystals of **2** were obtained in 24 h from the filtrate. Isolated yield: 75%. Anal. Calcd for **2**, $C_{20}H_{30}N_{30}Cu_4$: C, 25.42; H, 3.20; N, 44.47. Found: C, 25.59; H, 3.34; N, 44.41. IR (KBr, cm^{-1}): 2020, 2054, and 2069 for the azido groups.

*Synthesis of the Complex $[Cu_4(N_3)_8(L^3)_2]_n$ (**3**).* The rod-shaped black crystals of **3** were obtained in 24 h by a method similar to that described above for complex **2**, using *N*,*N*-deen (1 mmol, 116 mg) instead of *N*,*N*-dmen. Isolated yield: 47%. Anal. Calcd for **3**, $C_{24}H_{38}N_{30}Cu_4$: C, 28.80; H, 3.83; N, 41.98. Found: C, 28.72; H, 3.77; N, 41.81. IR (KBr, cm^{-1}): 2030 and 2064 for the azido groups.

*Synthesis of the Complex $[Cu_9(N_3)_{18}(L^4)_4]_n$ (**4**).* The rectangular black crystals of **4** were obtained in 24 h by a method similar to that described above for complex **2**, using *N*,*N*,2,2-tmpn (1 mmol, 130 mg) instead of *N*,*N*-dmen. Isolated yield: 42%. Anal. Calcd for **4**, $C_{52}H_{84}N_{66}Cu_9$: C, 28.32; H, 3.84; N, 41.91. Found: C, 28.28; H, 3.79; N, 41.95. IR (KBr, cm^{-1}): 2022, 2051, and 2080 for the azido groups.

X-ray Crystallographic Data Collection and Refinements. Single-crystal X-ray data for all four complexes were collected on a Bruker SMART APEX CCD diffractometer using the *SMART/SAINT* software.[12] Intensity data were collected using graphite-monochromatized Mo Kα radiation (0.710 73 Å) at 293 K. The structures were solved by direct methods using the *SHELX-97*[13] program incorporated into *WinGX*.[14] Empirical absorption corrections were applied with *SADABS*.[15] All non-hydrogen atoms were refined with anisotropic displacement coefficients (except for **4**, for which two nitrogen atoms of an azido group were found to be disordered). The hydrogen atoms bonded to carbon were included in geometric positions and given thermal parameters equivalent to 1.2 times those of the atom to which they were attached. Structures were drawn using ORTEP-3 for Windows.[16] Crystallographic data and refinement parameters are given in Table 1, and important interatomic distances and angles are given in Table 2 (for **1** and **2**) and 3 (for **3** and **4**).

COMPUTATIONAL METHODOLOGY

The exchange coupling constants in the reported complexes (**1**−**3**) have been calculated using the following computational methodology.[17−20] Using a phenomenological Heisenberg Hamiltonian $H = -\sum_{i>j} J_{ij} S_i S_j$ (where where S_i and S_j are the spin operators of the paramagnetic metal centers i and j and the J_{ij} parameters are the exchange coupling constants for the different pairwise interactions between the paramagnetic metal centers of the molecule) to describe the exchange coupling between each pair of transition-metal ions present in the polynuclear complex, the full Hamiltonian matrix for the entire system can be constructed.

To calculate the exchange coupling constants for any polynuclear complex with n different exchange constants, at least the energy of $n+1$ spin configurations must be calculated. In the case of the studied tetranuclear complexes, the exchange coupling values J_1 and J_2 were obtained by taking into account the energy of three different spin distributions: quintet with $S = 2$, triplet with $S = 1$, and singlet with $S = 0$.

The hybrid B3LYP functional[21] has been used in all calculations, as implemented in the *Gaussian 03* package,[22] mixing the exact Hartree−Fock-type exchange with Becke's expression for the exchange functional[23] and that proposed by Lee−Yang−Parr for the correlation contribution.[24] The use of

dx.doi.org/10.1021/ic102580a |*Inorg. Chem.* 2011, 50, 3621–3631

Scheme 2. Graphical Representation of a Possible Reaction Pathway for the Formation and Trapping of L^1

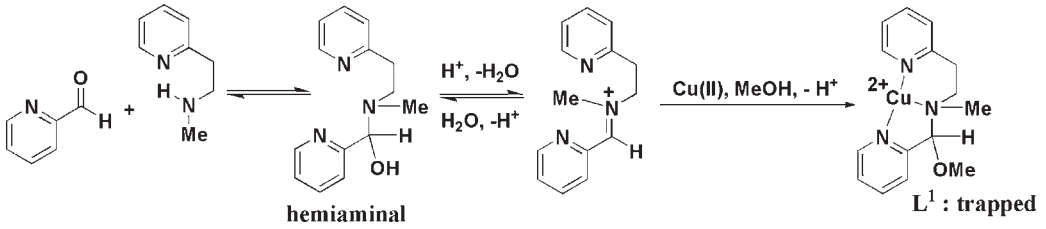

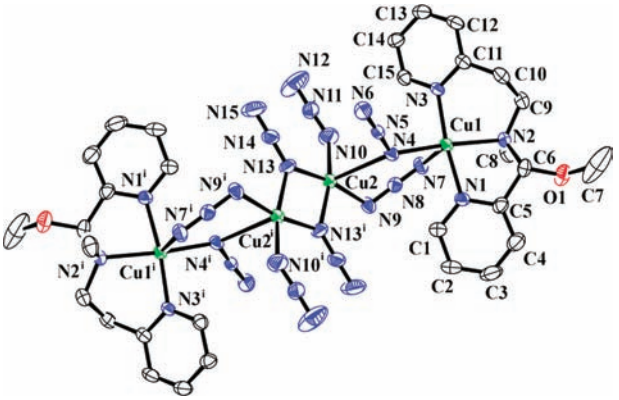

Figure 1. ORTEP view of the basic unit of **1**. Hydrogen atoms have been removed for clarity. Thermal ellipsoids are at the 30% probability level.

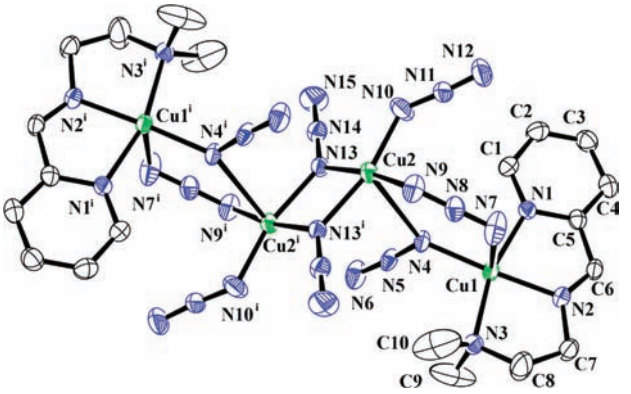

Figure 2. ORTEP view of the basic unit of **2**. Hydrogen atoms have been removed for clarity. Thermal ellipsoids are at the 30% probability level.

the nonprojected energy of the broken-symmetry solution as the energy of the low-spin state within the DFT framework provides more or less satisfactory results, avoiding cancellation of the nondynamic correlation effects.[25] The broken-symmetry approach along with electron correlations at the B3LYP level has been widely used to investigate the magnetic properties in a large number of magnetic systems. We have considered the LanL2DZ basis set for all atoms. All of the energy calculations were performed including a 10^{-8} density-based convergence criterion.

RESULTS AND DISCUSSION

Synthesis. All four complexes were obtained from the reaction of $Cu(NO_3)_2 \cdot 3H_2O$ and 0.5 mol equiv of chelating tridentate ligands, formed in situ, with an excess of NaN_3 in a $MeOH/H_2O$ mixture. It is well established in the literature that the excess of NaN_3 prevents immediate precipitation and allows crystallization of multidimensional compounds via the self-assembly of smaller units. The ligands L^2, L^3, and L^4 are simple condensation products (imines) of an aldehyde and a primary amine (actually diamines, with one primary nitrogen atom and one tertiary nitrogen atom), formed by elimination of a water molecule. However, L^1 requires a little more attention because the amine used for condensation is secondary. Secondary amines normally react with aldehydes to form an unstable hemiaminal, which can later eliminate a water molecule to form an enamine. However, in this case, deprotonation leading to an enamine is not possible because of the lack of an α-hydrogen atom. The source of the methoxy group in L^1 (which is a hemiaminal ether) is thus the excess of MeOH present in the reaction mixture. Several attempts to isolate L^1 failed, which is not surprising because it is well-known in the literature that the hemiaminal ethers are generally very labile (unstable in both acidic and basic solutions, as well as very highly temperature-sensitive, with the equilibrium lying almost entirely toward the starting materials), and only a few cyclic or protected compounds have been characterized.[26] It is interesting to note that for **2**−**4** the reaction can be carried out at room temperature (after the condensation step), but we were unable to isolate **1** in this way. Furthermore, **2**−**4** can also be obtained (in comparable yields as described in the synthesis section) by heating the reaction mixture as in the case of **1**. So, the ligand L^1 can be considered as a trapped unstable intermediate. Complex **1** represents a unique example where the so-called unstable hemiaminal ether (L^1) has been isolated in metal-arrested form. Scheme 2 shows a simplified way of forming and trapping L^1 (may not be the actual reaction mechanism). Nevertheless, formation of the hemiaminal ether moiety is very interesting and will be explored in detail elsewhere.

Intense and broad multiple IR absorptions of azido stretching vibrations in the range from 2020 to 2080 cm^{-1} are consistent with the presence of various bonding modes of the bridging azido ligands.

Structure Description of ***1*** *and* ***2***. The crystal structures of complexes **1** and **2** reveal remarkably similar one-dimensional (1D) arrangements consisting of tetranuclear building units (Figures 1 and 2), although the space groups in which they crystallize are different (Table 1). The asymmetric units consist of two metal atoms, one tridentate L^1 or L^2 ligand, and four azido anions. The tridentate ligands coordinate to one of the Cu^{II} atoms (Cu1, having a distorted octahedral geometry) and the other metal (Cu2, having a square-pyramidal coordination environment) has only azido anions in its coordination sphere. The symmetry of both crystals allows two Cu2 atoms to join together by azido bridges to form the basic tetranuclear unit. Cu1 has three nitrogen atoms from the blocking ligand and one $\mu_{1,1}$-nitrogen atom of an azido group (joining it with the adjacent

dx.doi.org/10.1021/ic102580a |*Inorg. Chem.* 2011, 50, 3621–3631

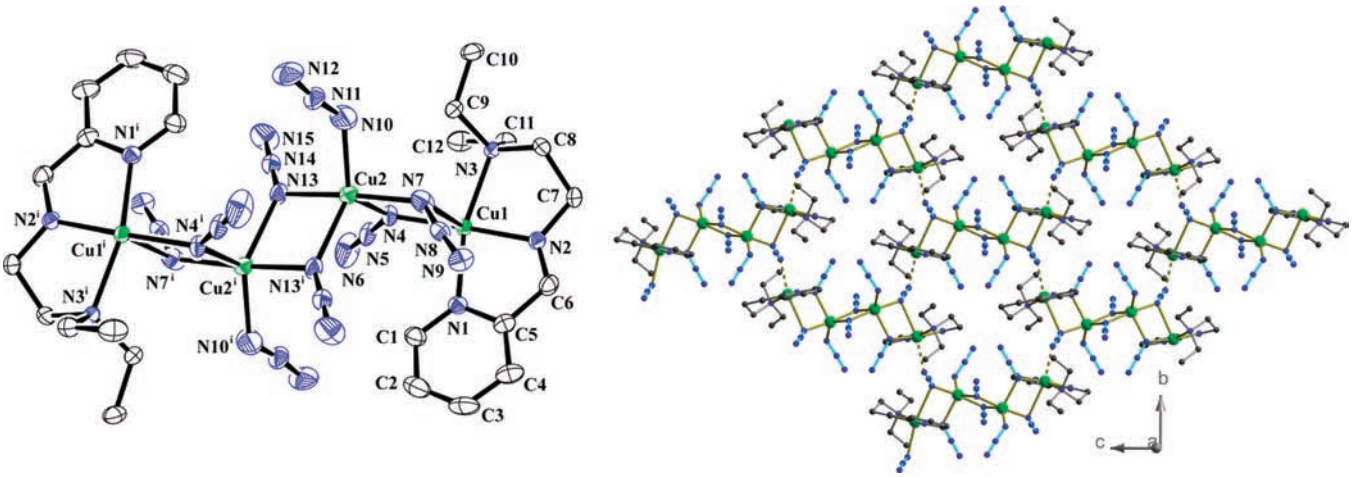

Figure 3. ORTEP view of the basic unit of **3** (left). Thermal ellipsoids are at the 30% probability level. Ball-and-stick representation of the 2D chain of **3**. Color code: copper, green; nitrogen, blue; carbon, gray. Hydrogen atoms have been removed for clarity (right).

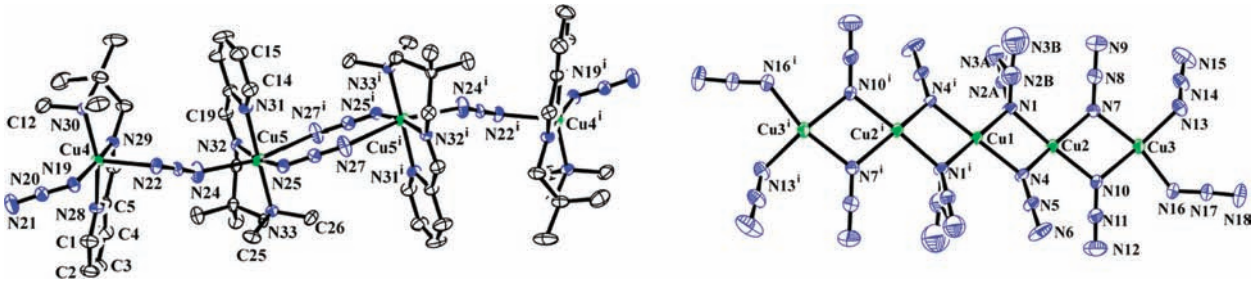

Figure 4. ORTEP views of the two fragments of the basic unit of **4**. Thermal ellipsoids are at the 30% probability level. Hydrogen atoms have been removed for clarity.

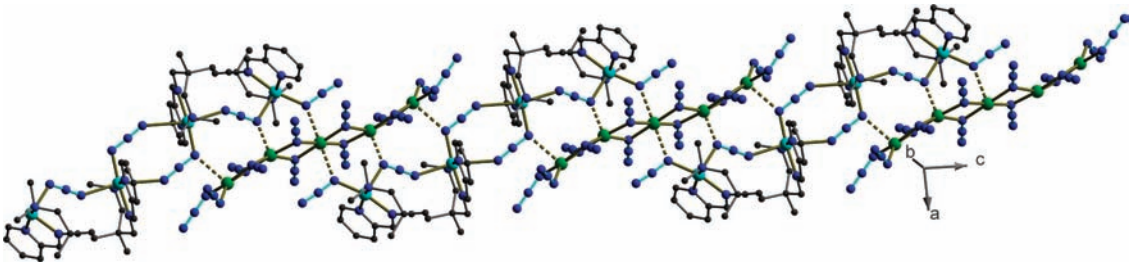

Figure 5. Ball-and-stick representation of the 1D arrangement of **4**. Color code: copper, green/cyan; nitrogen, blue; carbon, gray. Hydrogen atoms have been removed for clarity.

metal atom in an EO fashion) in its equatorial sites [Cu1−N_{eq}, 1.973(4)/1.961(4)−2.097(4)/2.068(4) Å, from here on the parameters regarding **1** and **2** are given in the format **1**/**2**]. The axial nitrogen atoms are provided by one $\mu_{1,3}$-azido [Cu1−N7, 2.579(5)/2.645(5) Å] group and one $\mu_{1,1,3}$-azido group [Cu1−N6, 2.899(5)/2.645(5) Å] from an adjacent tetranuclear unit. In the basal plane of Cu2, there are two $\mu_{1,1}$-nitrogen atoms from two EO azido bridges (which join it to a neighboring Cu2 atom), a nitrogen atom from a $\mu_{1,3}$-azido group, and a nitrogen atom from a pendant azido group [Cu2−N_{bas}, 1.915(5)/1.930(5)−2.005(4)/2.020(4) Å], while the apical nitrogen is provided by an EO azido group bridging to an adjacent Cu1 atom [Cu2−N4, 2.689(4)/2.641(4) Å]. Thus, Cu1 is bridged to Cu2 by one EO and one EE azido group, and Cu2 is connected to its adjacent Cu2 by two EO azido bridges, forming the tetranuclear unit. The coexistence of EO and EE azido bridges between a pair of metal centers (Cu1 and Cu2) is unusual because the EO mode pulls the metals closer while a wide separation is preferred in the EE bridging pathway. Each unit joins to its neighboring unit by two $\mu_{1,1,3}$-azido bridges, and the chain formed runs along the crystallographic *a* axis (Figure S2 in the Supporting Information).

Within the Cu_4^{II} units, the Cu1−Cu2 distance [4.293(1)/4.255(1) Å] is larger than that for Cu2−Cu2 [3.121(1)/3.161(1) Å], while the two nearest Cu1 atoms from the adjacent units are separated by 5.687(1)/5.409(1) Å. The EO bridging angles Cu1−N4−Cu2 [131.1(2)/134.7(2)°] and Cu2−N1-3−Cu2 [103.4(2)/103.3(2)°] are almost equal in the two

dx.doi.org/10.1021/ic102580a |*Inorg. Chem.* 2011, 50, 3621–3631

complexes. However, the torsion angles involving the EE azido group bridging Cu1 and Cu2 vary widely (Cu1−N7−N9−Cu2, −52.80° for **1** and −20.09° for **2**), probably because of the differences in the geometrical and steric constraints of the two different ligands. For L^1, the three nitrogen donor atoms N1, N2, and N3 have sp^2, sp^3, and sp^2 hybridizations, respectively, while those in L^2 have sp^2, sp^2, and sp^3 arrangements, respectively. The total bite angles of the two ligands also differ considerably (N1−Cu1−N3, 173.1° for **1** and 163.4° for **2**). In effect, the N6 atom (of the EO azido group that joins Cu1 and Cu2) in **2** comes very close in space [Cu2−N6, 3.003(5) Å] at the sixth coordination position of an otherwise square-pyramidal Cu2 atom. However, for **1**, the Cu2−N6 distance is too large [4.667(5) Å] to have any bonding interaction.

Examples of the coexistence of both EO and EE azido bridges between two copper atoms are limited.[8g,h] Generally the EO mode is converging in nature and brings two bridged metal centers very close (ca. 3 Å), while the three-atom EE mode prefers the metals at greater separations (ca. 5 Å). In this situation, the EO mode needs to involve at least one longer bond (axial) and the bridging angle also expands. For both **1** and **2**, the Cu1−Cu2 distance is ca. 4.2 Å and the EO bridging angle is greater than 130°. To the best of our knowledge, the Cu1−N_{EO}−Cu2 angle for **2** (134.7°) is the largest for this kind of bridging.

Structure Description of ***3***. **3** crystallizes in the monoclinic space group $P2_1/n$ and like the previous two complexes contains a Cu^{II}_4 basic unit (Figure 3). However, the bridging arrangement between the peripheral copper atoms is different in **3**, and unlike **1** and **2**, it has an overall two-dimensional (2D) structure. The asymmetric unit contains two metal atoms (Cu1, which has a tetragonally distorted octahedral geometry, and Cu2, which has a highly distorted square-pyramidal coordination geometry), one tridentate ligand L^3, and four azido anions. All of the azido groups linking the metals within the basic unit are EO in nature (unlike **1** and **2**). Cu1 has three nitrogen atoms from the ligand L3 and a $\mu_{1,1}$-nitrogen atom (linking to Cu2) in its equatorial plane [Cu1−N_{eq}, 1.951(2)−2.123(2) Å], while the axial sites contain one η^1-nitrogen atom and one η^2-nitrogen atom of two $\mu_{1,1,3}$ azido groups [Cu1−N_{ax}, 2.383(3)−2.610(5) Å]. The approximate basal plane of Cu2 consists of two EO azido nitrogen atoms (linking to a neighboring Cu2 atom within the basic unit), one η^2-nitrogen atom of a $\mu_{1,1,3}$-azido group (linking to a Cu1 atom within the unit), and a nitrogen atom from a pendant azido group [Cu2−N_{bas}, 1.975(4)−2.128(3) Å], while the apical position is taken up by another $\mu_{1,1}$-nitrogen atom [Cu2−N4, 2.208(2) Å] of an EO azido group (linking to Cu1). The double EO azido bridge between the two central Cu2 atoms of the basic tetranuclear unit is symmetrical in nature, with the two Cu2−N_{EO}−Cu2 angles being equal to 101.29(12)°, while the same for the peripheral atoms (Cu1 and Cu2) is asymmetric, with the two different Cu1−N_{EO}−Cu2 angles measuring at 93.60(11)° and 108.60(11)°.

Each of these Cu^{II}_4 units is linked to four such adjacent units through four $\mu_{1,1,3}$-azido bridges and thus forms an overall 2D structure (Figure 3).

Structure Description of ***4***. This complex crystallizes in the triclinic space group $P\bar{1}$ and has a complicated 1D structure with Cu^{II}_9 repeating units. The Cu^{II}_9 basic unit can be broken down into two centrosymmetric fragments, a linear tetranuclear unit, $[Cu_4(L^4)_4(N_3)_6]^{2+}$, in which all copper atoms have the L^4 ligated to them (Figure 4), and a linear pentanuclear unit, $[Cu_5(N_3)_{12}]^{2-}$, in which the copper atoms have only azido anions in their coordination spheres. In the tetranuclear unit, the copper atoms are joined by only EE azido groups, while in the pentanuclear unit, all copper atoms are linked by double EO azido bridges. The pentanuclear unit has three crystallographically independent copper atoms, among which the central Cu1 atom has a distorted octahedral geometry, while the other two metal atoms are (Cu2 and Cu3) square-pyramidal in nature.

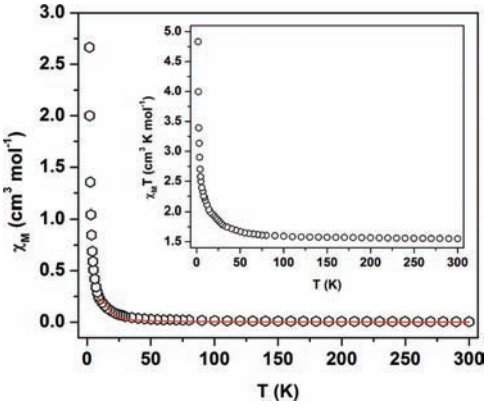

Figure 6. Plots of χ_M vs T and $\chi_M T$ vs T (inset) for complex **1** in the temperature range of 1.8−300 K. The red line indicates the fitting using the theoretical model (see the text).

Scheme 3. Schematic Diagrams Representing the Exchange Interaction Models Used for Complexes 1 and 2 (Left) and Complex 3 (Right)

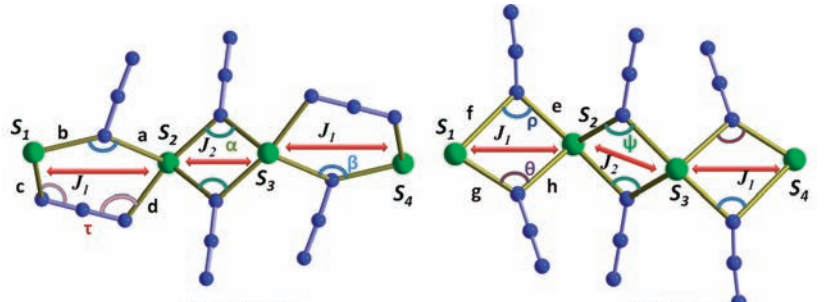

Complex 1/2
α=103.4/103.3°, β=131.1/134.7°, τ=-52.8/-20.1°(torsion)
a=2.69/2.64, b=2.02/1.96, c=2.58/2.64, d=1.98/1.97 Å

Complex 3
Ψ=101.3°,θ=108.6°,ρ=93.6°.
e=2.00, f=2.61, g=1.96, h=2.21Å.

dx.doi.org/10.1021/ic102580a |*Inorg. Chem.* 2011, 50, 3621–3631

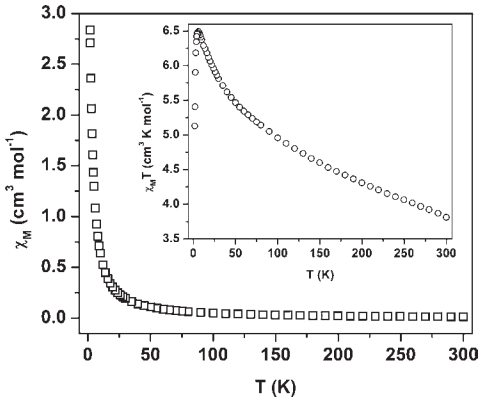

Figure 7. Plots of χ_M vs T and $\chi_M T$ vs T (inset) for complex **4** in the temperature range of 1.8−300 K.

All six coordination sites of Cu1 are taken up by $\mu_{1,1}$-nitrogen atoms of six EO azido bridges, of which the equatorial nitrogen atoms join two neighboring Cu2 atoms [Cu1−N_{eq}, 1.990(2)−1.999(2)Å] and the axial nitrogen atoms link to the Cu4 atoms in the two adjacent tetranuclear units [Cu1−N_{ax}, 2.591(2) Å]. The basal plane of the Cu2 atom is occupied by four $\mu_{1,1}$-nitrogen atoms of four EO azido groups [Cu2−N_{ap}, 1.974(2)−2.022(2) Å], and the apical position is taken up by a η^2-nitrogen atom (linking to a Cu4 atom of an adjacent Cu^{II}_4 unit) of a $\mu_{1,1,3}$-azido group [Cu2−N22, 2.263(2) Å]. The Cu3 atom has two EO azido nitrogen atoms and two pendant azido nitrogen atoms in its basal plane [Cu3−N_{bas}, 1.953(3)−2.015(2) Å], while the apical position is taken up by a η^2-nitrogen atom (linking to a Cu5 atom of an adjacent Cu^{II}_4 unit) of a $\mu_{1,1,3}$-azido group [Cu3−N25, 2.663(2) Å].

The Cu^{II}_4 unit has two crystallographically different copper atoms; the two peripheral Cu4 atoms have a square-pyramidal geometry, while the two central Cu5 atoms are distorted octahedral in nature. Within this tetranuclear unit, Cu4 is linked to the neighboring Cu5 atom by a single EE azido group, while the two Cu5 atoms are linked by double EE azido bridges. Three nitrogen atoms from the ligand L^4 and a nitrogen atom of an EO azido group occupy the basal plane of Cu4 [Cu4−N_{bas}, 1.989(2)−2.070(2) Å], while the apical position is taken up by a nitrogen atom of an EE azido group [Cu4−N22, 2.242(2) Å]. For Cu5, the equatorial plane is taken up by three nitrogen atoms from the tridentate ligand and a η^2-nitrogen atom (linking to a Cu3 atom of an adjacent Cu^{II}_5 unit) of a $\mu_{1,1,3}$-azido group [Cu5−N_{eq}, 1.987(2)−2.059(2) Å], while the axial positions have two η^1-nitrogen atoms of two $\mu_{1,1,3}$-azido groups [Cu5−N_{ax}, 2.447(3)−2.729(3) Å]. Thus, the two adjacent Cu^{II}_4 and Cu^{II}_5 units are joined together by one $\mu_{1,1}$-azido and two $\mu_{1,1,3}$-azido groups, and the process repeats to form a 1D arrangement along the crystallographic c axis (Figure 5).

Magnetic Behavior. *Complexes **1** and **2**.* The close similarities in the structures of **1** and **2** are also reflected in their magnetic behavior (Figure 6 and the Supporting Information). The room temperature (300 K) $\chi_M T$ values [1.59 (**1**)/1.76 (**2**) cm^3 K mol^{-1}] are slightly higher than that for four uncoupled Cu^{II} ions ($\chi_M T$ = 0.375 cm^3 K mol^{-1} for an $S = {}^1/_2$ ion with $g = 2$). For both complexes, the $\chi_M T$ value gradually increases upon a decrease in the temperature from 300 K, and below 50 K, there is a sharp jump, and finally it reaches a maximum value of 4.83 (**1**)/5.58 (**2**) cm^3 K mol^{-1} at 1.8 K. The $1/\chi_M$ vs T plot (300−50 K) obeys the Curie−Weiss law with a positive Weiss constant of θ = 5.03 (**1**)/16.40 (**2**) K (Figure S5 in the Supporting Information). The nature of the $\chi_M T$ vs T plot and the positive θ suggest a dominant ferromagnetic exchange among the four Cu^{II} ions through the azido bridges.

Table 4. Comparison of the Experimental and DFT Studies

complex	J_i	from fitting (cm^{-1})	from DFT (cm^{-1})
1	J_1	−2.2	−31.7
	J_2	+55.1	+105.7
2	J_1	−1.4	−22.7
	J_2	+39.3	+56.7
3	J_1	−1.9	−13.6
	J_2	+27.2	+54.4

Scheme 4. Systems Used for Computational Studies on 2

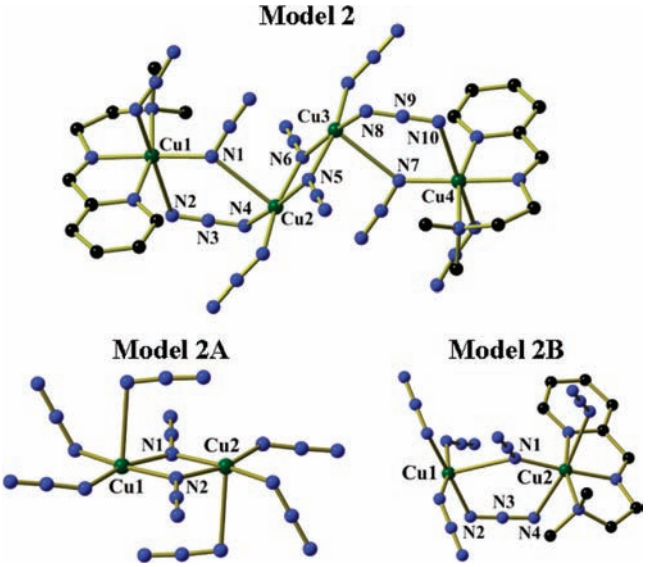

The magnetic exchange in the basic centrosymmetric core can be modeled as $Cu(S_1) - J_1 - Cu(S_2) - J_2 - Cu(S_3) - J_1 - Cu(S_4)$, and because the two central copper atoms are bridged by double EO azido bridges while the peripheral copper atoms are bridged by one EO azido group and one EE azido group, J_1 and J_2 are not expected to be identical (Scheme 3).[27,10d] A reasonable fit can be obtained for interaction of the tetranuclear units by application of the conventional Hamiltonian

$$H = -J_1(S_1S_2 + S_3S_4) - J_2S_2S_3$$

and the introduction of an intertrimer zJ' term. Considering these three different exchange parameters, analysis of the experimental susceptibility values has been performed using the following expression:

$$\chi_M = \chi_M'/[1 - \chi_M'(2zJ'/Ng^2\beta^2)]$$

$$\chi_M' = (Ng^2\beta^2/3kT)(A/B)$$

where $A = 30\exp(E_1/kT) + 6\exp(E_2/kT) + 6\exp(E_3/kT) + 6\exp(E_4/kT)$ and $B = 5\exp(E_1/kT) + 3\exp(E_2/kT) + 3\exp(E_3/kT) + 3\exp(E_4/kT) + \exp(E_5/kT) + \exp(E_6/kT)$.

$$E_1 = J_1/2 + J_2/4$$

dx.doi.org/10.1021/ic102580a |*Inorg. Chem.* 2011, 50, 3621–3631

$$E_2 = -J_1/2 + J_2/4$$

$$E_3 = -J_2/4 - ({J_1}^2 + {J_2}^2)^{1/2}/2$$

$$E_4 = -J_2/4 + ({J_1}^2 + {J_2}^2)^{1/2}/2$$

$$E_5 = -J_1/2 - J_2/4 - (4{J_1}^2 - 2J_1J_2 + {J_2}^2)^{1/2}/2$$

$$E_6 = -J_1/2 - J_2/4 + (4{J_1}^2 - 2J_1J_2 + {J_2}^2)^{1/2}/2$$

The values giving the best fit (10−300 K) for **1** are $J_1 = -2.2(1)$ cm^{-1}, $J_2 = +55.1(7)$ cm^{-1}, $zJ' = -1.7(2)$ cm^{-1}, and $g = 2.15(1)$ ($R = 8.8 \times 10^{-5}$), and those for **2** are $J_1 = -1.4(1)$ cm^{-1}, $J_2 = +39.3(6)$ cm^{-1}, $zJ' = -1.0(2)$ cm^{-1}, and $g = 2.12(1)$ ($R = 7.3 \times 10^{-5}$).

In both complexes, the two central Cu^{II} ions of the linear Cu_4 basic units are in square-pyramidal environments, whereas the peripheral Cu^{II} ions have octahedral geometries. The longer axial bond lengths in both cases indicate the presence of the unpaired electron in the basal/equatorial $d_{x^2-y^2}$ orbital. The Cu−N_{EO}−Cu bond angles for the two central metal atoms (for both complexes) are well below the cutoff angle 108°, and also all bridging bonds are "short" in nature. So, a moderately strong ferromagnetic interaction is expected for this pair of copper ions and is indeed found from the fitting [J_2 = +55 (**1**)/+39 (**2**) cm^{-1}], whereas the Cu−N_{EO}−Cu bond angle between the other pair is very high [131.1° (**1**)/134.7° (**2**)] and this pair is also linked by an EE azido group, which generally transmits antiferromagnetic interaction. Because both bridges for this pair involve axial−equatorial exchange interactions, the low negative fitting value obtained matches well with our expectations. The intercluster antiferromagnetic interaction is probably a result of *cis*-EE pathways.

Complex ***3***. At 300 K, the $\chi_M T$ value is 1.56 cm^3 K mol^{-1}, which is a little higher than expected for four uncoupled Cu^{II} ions (Figure S4 in the Supporting Information). The $\chi_M T$ value gradually increases upon a decrease in the temperature and shows a rapid jump below 50 K, to reach a maximum value of 1.97 cm^3 K mol^{-1} at 14 K. Below this temperature, the $\chi_M T$ value decreases sharply (saturation effect) to 1.26 cm^3 K mol^{-1} at 1.8 K. The $1/\chi_M$ vs T plots (300−50 K) obey the Curie−Weiss law (Supporting Information) with a positive Weiss constant of $\theta = +13.77$ K, which along with the nature of the $\chi_M T$ vs T plot indicates a dominant ferromagnetic interaction among the metal ions.

The Cu^{II}_4 building unit of **3** can be treated similarly to that of **1** and **2** (Scheme 3), and thus the same model can be used to fit the magnetic susceptibility data. The values giving the best fit (10−300 K) are $J_1 = -1.9(1)$ cm^{-1}, $J_2 = +27.2(8)$ cm^{-1}, $zJ' = -1.5(1)$ cm^{-1}, and $g = 2.11(1)$ ($R = 6.6 \times 10^{-5}$).

For **3**, the two central copper ions are in a distorted square-pyramidal geometry, but the bond parameters suggest that the bridging between this pair of metal atoms is otherwise very much similar to that of **1** and **2**. The peripheral copper atoms, however, are bridged by double (asymmetric) EO azido groups, with the two Cu−N_{EO}−Cu bridging angles on both sides of the cutoff angle (108.6 and 93.6°). The bridging bonds involving the larger angle are smaller (equatorial−apical) than the bonds (axial−basal) involving the shorter angle (Scheme 3). Thus, the antiferromagnetic interaction (108.6°, with short bonds; nd_{avg} = 2.08 Å) is stronger than the ferromagnetic interaction (93.6°, with longer bonds; d_{avg} = 2.31 Å), giving an overall small negative value for J_1.

Complex ***4***. The temperature dependence of the magnetic susceptibility of **4** in the form of $\chi_M T$ and χ_M vs T is displayed in Figure 7 (where χ_M is the molar magnetic susceptibility per Cu^{II}_9 unit). At room temperature, the value of $\chi_M T$ is 3.81 cm^3 K mol^{-1}, which is slightly above the expected value of 3.38 cm^3 K mol^{-1} for nine uncoupled Cu^{II} ions. Upon cooling, the $\chi_M T$ value increases slowly and then more rapidly below 75 K to reach the maximum value of 6.49 cm^3 K mol^{-1} at 6 K and then falls rapidly to 5.12 cm^3 K mol^{-1} at 1.8 K, indicating a ferromagnetic coupling between the Cu^{II} ions. Accordingly, the $1/\chi_M$ vs T plot (300−50 K) follows the Curie−Weiss law (Figure S5 in the Supporting Information) with a positive Weiss constant of $\theta = +24.91$ K.

Unfortunately, we were not able to model the exchange pathways because of the complicated structure of the complex and a basic unit of high nuclearity, which leads to overparametrization. The ferromagnetic exchange within the complex is dominant because the Cu^{II}_5 unit is expected to be very strongly

Table 5. Atomic Spin Densities (in au) of 2 in Its Three Spin States

atom	quintet	triplet	singlet
Cu1	0.496 727	0.522 840	0.510 389
Cu2	0.494 519	0.518 581	−0.322 628
Cu3	0.503 729	0.519 932	0.329 160
Cu4	0.492 239	−0.540 176	−0.510 563
N1	0.134 774	0.130 965	0.128 922
N2	0.114 448	0.106 334	−0.065 606
N3	−0.023 018	−0.017 885	−0.001 011
N4	0.045 473	0.037 738	−0.038 617
N5	0.110 300	0.105 357	−0.011 659
N6	0.110 145	0.105 925	0.007 452
N7	0.140 195	−0.118 975	−0.125 910
N8	0.043 261	0.033 519	0.042 287
N9	−0.020 048	−0.015 444	−0.001 272
N10	0.109 200	0.102 818	0.070 392

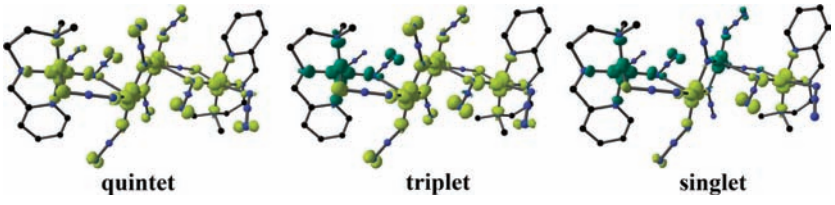

Figure 8. Spin-density maps calculated for model **2** at the B3LYP level for the three states. Positive and negative spin populations are represented as yellow and green surfaces. The isodensity surfaces correspond to a value of 0.0025 e/b^3.

dx.doi.org/10.1021/ic102580a |*Inorg. Chem.* 2011, 50, 3621–3631

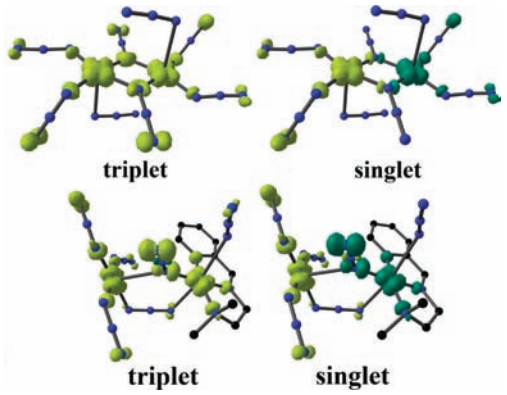

Figure 9. Spin-density maps calculated for **2A** (top) and **2B** (bottom) at the B3LYP level for singlet and triplet states. Positive and negative spin populations are represented as yellow and green surfaces. The isodensity surfaces correspond to a value of 0.0025 e/b^3.

ferromagnetically coupled by the EO azido bridges (the average Cu−N_{EO}−Cu bridging angle is 101.3°).

Theoretical Study. To gain insight into the magnetic exchange mechanism in complexes **1**−**3**, spin-unrestricted calculations were performed at the X-ray geometry using the *Gaussian 03* package at the B3LYP level employing the LanL2DZ basis set. The results of the theoretical studies (see the Computational Methodology section for details) in terms of the calculated exchange parameters are summarized in Table 4.

For all three complexes, the quintet state is found to be the ground state, followed by the triplet and singlet states, respectively. The *J* values were calculated using the energy differences of these states as described earlier.

Because all three complexes present similar features in terms of the relative energies of their spin states, here we will give a detailed description for **2**, and the same for the other two complexes is presented in the Supporting Information. To further ascertain the accuracy of the exchange parameter values, we have performed single-point energy calculations (singlet and triplet states) of the two dinuclear fragments of the tetranuclear unit to determine individually the pairwise exchange coupling constants (models **2A** and **2B**, Scheme 4). The calculated values for the exchange parameters J_1 and J_2 from the two fragments are −18.1 and +44.1 cm^{-1}, respectively, and are in good agreement with the values calculated for the tetranuclear model (see Table 4).

The representations of the spin-density distribution corresponding to three spin states for **2** are plotted in Figure 8, and the atomic spin densities of the four Cu^{II} atoms and the bridging N atoms of the three states are summarized in Table 5. As expected, the spin-density distributions for the two central metal atoms in the quintet ground states in **2** and **2A** (Figure 9) show predominance of the delocalization mechanism through a σ-type exchange pathway involving the $d_{x^2-y^2}$ magnetic orbitals of the Cu^{II} atoms and the sp^2 hybrid orbitals of the EO azido nitrogen bridging atoms, providing evidence for the moderately strong positive exchange observed experimentally. For **2**, the spin densities delocalized over the nitrogen bridging atoms (N5 and N6) are around 0.11 e, and the average spin population on the Cu^{II} atoms (Cu2 and Cu3) is 0.50 e (see Table 5). Spin-density distributions for complexes **1** and **3** also show similar features (see the Supporting Information).

Although the agreement in the sign and magnitude order between the theoretical and experimental results for the three complexes is fairly good, the *J* values obtained by DFT calculations are considerably higher than the experimental ones. This may be attributed to either the intrinsic limitations of the method, the flexibility of the structures that allow structural changes when the sample is cooled, or simply the fact that the basic units are not magnetically isolated, as indicated by the intercluster exchange parameter.

CONCLUDING REMARKS

We have presented versatility of azide as a linker using lower molar amounts (0.5 equiv with respect to copper) of the blocking ligands, by introducing four tridentate ligands to synthesize and characterize four polyclusters. All four complexes were found to be predominantly ferromagnetic, and the results of the theoretical treatment (DFT) corroborated nicely with the experimental findings. The chelating ligands were prepared in situ by simple condensation reactions. Interestingly, in **1**, the blocking ligand, which is a new hemiaminal ether, was found to be "trapped". Although hemiaminal ethers are known to be very unstable intermediates, complex **1** represents a unique stable system containing trapped hemiaminal ether L[1]. Although the two tridentate ligands in **1** and **2** are structurally different, the basic and overall structures (1D) of these two complexes were found to be remarkably similar, whereas for **2** and **3**, the two ligands differ only by the alkyl (Me/Et) groups on one of the nitrogen atoms, and results in the two are very different in both basic repeating unit and overall structures. Like most of the serendipitous assemblies, no conclusive explanation is available for these observations, and probably this inadequacy fuels the surge for new reaction methodologies and, in turn, new structures.

ASSOCIATED CONTENT

Supporting Information. X-ray crystallographic data in CIF format, views of 1D structures of **1** and **2**, powder XRD patterns, temperature-dependent susceptibility data for **2** and **3**, Curie−Weiss fittings of the $1/\chi_M$ vs *T* data, *M* vs *H* plots of **1**−**4**, and atomic spin densities of the models used for the DFT study. This material is available free of charge via the Internet at http://pubs.acs.org.

AUTHOR INFORMATION

Corresponding Author

*E-mail: psm@ipc.iisc.ernet.in. Tel: 91-80-22933352. Fax: 91-80-23601552.

ACKNOWLEDGMENT

S.M. gratefully acknowledges the Council of Scientific and Industrial Research, New Delhi, India, for the award of a Research Fellowship. The authors sincerely thank Arun K. Bar for his help in single-crystal X-ray data collection and refinement. The authors also thank the Department of Science and Technology (DST), New Delhi, India, for financial support.

REFERENCES

(1) (a) O'Connor, C. J. *Research Frontiers in Magnetochemistry*; World Scientific: Singapore, 1993. (b) Christou, G.; Gatteschi, D.;

Hendrickson, D. N.; Sessoli, R. *MRS Bull.* **2000**, 66. (c) Jain, P.; Dalal, N. S.; Toby, B. H.; Kroto, H. W. *J. Am. Chem. Soc.* **2008**, *130*, 10450. (d) Winpenny, R. E. P. *Dalton Trans.* **2002**, 1. (e) Gatteschi, D.; Sessoli, R. *Angew. Chem., Int. Ed.* **2003**, *42*, 268. (f) Stamatatos, T. C.; Christou, A. G.; Jones, C. M.; O'Callaghan, B. J.; Abboud, K. A.; O'Brien, T. A.; Christou, G. *J. Am. Chem. Soc.* **2007**, *129*, 9840. (g) Vittal, J. J. *Coord. Chem. Rev.* **2007**, *251*, 1781. (h) Yoon, J.; Solomon, E. I. *Coord. Chem. Rev.* **2007**, *251*, 379. (i) Winpenny, R. E. P. *Angew Chem., Int. Ed.* **2008**, *47*, 7992. (j) Lee, C. F.; Leigh, D. A.; Pritcharg, R. G.; Schults, D.; Teat, S. J.; Timco, G. A.; Winpenny, R. E. P. *Nature* **2009**, *458*, 314. (k) Chandrasekhar, V.; Murugesapandian, B. *Acc. Chem. Res.* **2009**, *42*, 1047. (l) Chandrasekhar, V.; Murugesapandian, B.; Vittal, J. J.; Clérac, R. *Inorg. Chem.* **2009**, *48*, 1148. (m) Lama, P.; Aijaz, A.; Sanudo, C.; Bharadwaj, P. K. *Cryst. Growth Des.* **2010**, *10*, 283.

(2) (a) Rettig, S. J.; Storr, A.; Summers, D. A.; Thompson, R. C.; Trotter, J. *J. Am. Chem. Soc.* **1997**, *119*, 8675. (b) Lloret, F.; De Munno, G.; Julve, M.; Cano, J.; Ruiz, R.; Caneschi, A. *Angew. Chem., Int. Ed.* **1998**, *37*, 135. (c) Masciocchi, N.; Galli, S.; Sironi, A.; Barea, E.; Navarro, J. A. R.; Salas, J. M.; Tabares, L. *Chem. Mater.* **2003**, *15*, 2153.(d) Batten, S. R.; Murray, K. S. *Coord. Chem. Rev.* **2003**, *246*, 103 and references cited therein. (e) Tian, Y.-Q.; Cai, C.-X.; Ren, X.-M.; Duan, C.-Y.; Xu, Y.; Gao, S.; You, X.-Z. *Chem.—Eur. J.* **2003**, *9*, 5975.

(3) (a) Gole, B.; Chakrabarty, R.; Mukherjee, S.; Song, Y.; Mukherjee, P. S. *Dalton Trans.* **2010**, *39*, 9766. (b) Kwak, H. Y.; Ryu, D. W.; Lee, J. W.; Yoon, J. H.; Kim, H. C.; Koh, E. K.; Krinsky, J.; Hong, C. S. *Inorg. Chem.* **2010**, *49*, 4632. (c) Gil-Hernández, B.; Gili, P.; Vieth, J. K.; Janiak, C.; Sanchiz, J. *Inorg. Chem.* **2010**, *49*, 7478. (d) Mota, A. J.; Rodríguez-Diéguez, A.; Palacios, M. A.; Herrera, J. M.; Luneau, D.; Colacio, E. *Inorg. Chem.* **2010**, *49*, 8986. (e) Palacios, M. A.; Mota, A. J.; Perea-Buceta, J. E.; White, F. J.; Brechin, E. K.; Colacio, E. *Inorg. Chem.* **2010**, *49*, 10156. (f) Alborés, P.; Rentschler, E. *Inorg. Chem.* **2010**, *49*, 8953. (g) Cremades, E.; Ruiz, E. *Inorg. Chem.* **2010**, *49*, 9641. (h) Sarkar, S.; Datta, A.; Mondal, A.; Chopra, D.; Ribas, J.; Rajak, K. K.; Sairam, S. M.; Pati, S. K. *J. Phys. Chem. B* **2006**, *110*, 12.

(4) (a) Papaefstathiou, G. S.; Perlepes, S. P.; Escuer, A.; Vicente, R.; Font-Bardia, M.; Solans, X. *Angew. Chem., Int. Ed.* **2001**, *40*, 884. (b) Papaefstathiou, G. S.; Escuer, A.; Vicente, R.; Font-Bardia, M.; Solans, X.; Perlepes, S. P. *Chem. Commun.* **2001**, 2414. (c) Boudalis, A. K.; Donnadieu, B.; Nastopoulos, V.; Clemente-Juan, J. M.; Mari, A.; Sanakis, Y.; Tuchagues, J.-P.; Perlepes, S. P. *Angew. Chem., Int. Ed.* **2004**, *43*, 2266. (d) Nanda, P. K.; Aromí, G.; Ray, D. *Inorg. Chem.* **2006**, *45*, 3143. (e) Mandal, D.; Bertolasi, V.; Ribas-Ariño, J.; Ray, D. *Inorg. Chem.* **2008**, *47*, 3465. (f) Mukherjee, P.; Drew, M. G. B.; Gómez-García, C. J.; Ghosh, A. *Inorg. Chem.* **2009**, *48*, 5848. (g) Chattopadhyay, S.; Drew, M. G. B.; Diaz, C.; Ghosh, A. *Dalton Trans.* **2007**, 2492.

(5) (a) Naiya, S.; Biswas, C.; Drew, M. G. B.; Gómez-García, C. J.; Clemente-Juan, J. M.; Ghosh, A. *Inorg. Chem.* **2010**, *49*, 6616. (b) Biswas, C.; Drew, M. G. B.; Ruiz, E.; Estrader, M.; Diaz, C.; Ghosh, A. *Dalton Trans.* **2010**, *39*, 7474.

(6) (a) Kahn, O. *Chem. Phys. Lett.* **1997**, *265*, 165. (b) Thomas, L.; Lionti, F.; Ballou, R.; Gatteschi, D.; Sessoli, R.; Barbara, B. *Nature* **1996**, *383*, 145. (c) Sessoli, R.; Tsai, H.-L.; Schake, A. R.; Wang, S.; Vincent, J. B.; Folting, K.; Gatteschi, D.; Christou, G.; Hendrickson, D. N. *J. Am. Chem. Soc.* **1993**, *115*, 1804. (d) Shatruk, M.; Dragulescu-Andrasi, A.; Chambers, K. E.; Stoian, S. A.; Bominaar, E. L.; Achim, C.; Dunbar, K. R. *J. Am. Chem. Soc.* **2007**, *129*, 6104. (e) Tabellion, F. M.; Seidel, S. R.; Arif, A. M.; Stang, P. J. *J. Am. Chem. Soc.* **2001**, *123*, 11982. (f) Tolis, E. I.; Helliwell, M.; Langley, S.; Raftery, J.; Winpenny, R. E. P. *Angew Chem., Int. Ed.* **2003**, *42*, 3804.(g) Ribas, J.; Escuer, A.; Monfort; Vicente, R.; Cortés, R.; Lezama, L.; Rojo, T. *Coord. Chem. Rev.* **1999**, *193*−*195*, 1027 and references cited therein. (h) Maji, T. K.; Mukherjee, P. S.; Mostafa, G.; Mallah, T.; Cano-Boquera, J.; Chaudhuri, N. R. *Chem. Commun.* **2001**, 1012.

(7) (a) Mondal, K. C.; Song, Y.; Mukherjee, P. S. *Inorg. Chem.* **2007**, *46*, 9736. (b) Price, D. J.; Batten, S. R.; Moubaraki, B.; Murray, K. S. *Chem. Commun.* **2002**, 762. (c) Konar, S.; Zangrando, E.; Drew, M. G. B.; Mallah, T.; Ray Chaudhuri, N. *Inorg. Chem.* **2003**, *42*, 5966. (d) Müller, A.; Meyer, J.; Krickemeyer, E.; Beugholt, C.; Bögge, H.; Peters, F.; Schmidtmann, M.; Kögerler, P.; Koop, M. J. *Chem.—Eur. J.* **1998**, *4*, 1000. (e) Leibeling, G.; Demeshko, S.; Bauer-Siebenlist, B.; Meyer, F.; Pritzkow, H. *Eur. J. Inorg. Chem.* **2004**, 2413. (f) Demeshko, S.; Leibeling, G.; Dechert, S.; Meyer, F. *Dalton Trans.* **2006**, 3458.

(8) (a) Mukherjee, P. S.; Maji, T. K.; Mostafa, G.; Mallah, T.; Ray Chaudhuri, N. *Inorg. Chem.* **2000**, *39*, 5147. (b) Comarmond, J.; Plumere, P.; Lehn, J. M.; Agnus, Y.; Louis, R.; Weiss, R.; Kahn, O.; Morgesten-Badarau, I. *J. Am. Chem. Soc.* **1982**, *104*, 6330. (c) Kahn, O.; Sikorav, S.; Gouteron, J.; Jeannin, S.; Jeannin, Y. *Inorg. Chem.* **1983**, *22*, 2877. (d) Tandon, S. S.; Thompson, L. K.; Manuel, M. E.; Bridson, J. N. *Inorg. Chem.* **1994**, *33*, 5555. (e) Ribas, J.; Monfort, M.; Ghosh, B. K.; Solans, X.; Font-Bardía, M. *J. Chem. Soc., Chem. Commun.* **1995**, 2375. (f) Ribas, J.; Monfort, M.; Ghosh, B. K.; Solans, X. *Angew. Chem., Int. Ed. Engl.* **1994**, *33*, 2087. (g) Viau, G.; Lombardi, G. M.; De Munno, G.; Julve, M.; Lloret, F.; Faus, J.; Caneschi, A.; Clemente-Juan, J. M. *Chem. Commun.* **1997**, 1195. (h) Escuer, A.; Vicente, R.; Ribas, J.; El Fallah, M. S.; Solans, X.; Font-Bardia, M. *Inorg. Chem.* **1993**, *32*, 3727. (i) Ruiz, E.; Cano, J.; Alvarez, S.; Alemany, P. *J. Am. Chem. Soc.* **1998**, *120*, 11122. (j) Shen, Z.; Zuo, J.-L.; Gao, S.; Song, Y.; Che, C.-M.; Fun, H.-K.; You, X.-Z. *Angew. Chem., Int. Ed.* **2000**, *39*, 3633. (k) Hong, C. S.; Koo, J.; Son, S.-K.; Lee, Y. S.; Kim, Y.-S.; Do, Y. *Chem.—Eur. J.* **2001**, *7*, 4243.

(9) (a) Escuer, A.; Harding, C. J.; Dussart, Y.; Nelson, J.; McKee, V.; Vicente, R. *J. Chem. Soc., Dalton Trans.* **1999**, 223. (b) Escuer, A.; Font-Bardía, M.; Massoud, S. S.; Mautner, F. A.; Penalba, E.; Solans, X.; Vicente, R. *New J. Chem.* **2004**, *28*, 681. (c) Hong, C. S.; Do, Y. *Angew. Chem., Int. Ed.* **1999**, *38*, 193. (d) Mukherjee, P. S.; Dalai, S.; Zangrando, E.; Lloret, F.; Chaudhuri, N. R. *Chem. Commun.* **2001**, 1444. (e) Saha, S.; Koner, S.; Tuchagues, J.-P.; Boudalis, A. K.; Okamoto, K.-I.; Banerjee, S.; Mal, D. *Inorg. Chem.* **2005**, *44*, 6379. (f) Thompson, L. K.; Tandon, S. S.; Manuel, M. E. *Inorg. Chem.* **1995**, *34*, 2356. (g) Mautner, F. A.; Hanna, S.; Cortés, R.; Lezama, L.; Barandika, M. G.; Rojo, T. *Inorg. Chem.* **1999**, *38*, 4647. (h) Escuer, A.; Vicente, R.; El Fallah, M. S.; Goher, M. A. S.; Mautner, F. A. *Inorg. Chem.* **1998**, *37*, 4466.

(10) (a) Gu, Z.-G.; Zuo, J.-L.; You, X.-Z. *Dalton Trans.* **2007**, 4067. (b) Abu-Youssef, M. A. M.; Escuer, A.; Mautner, F. A. *Dalton Trans.* **2008**, 3553. (c) Gu, Z.-G.; Xu, Y.-F.; Yin, X.-J.; Zhou, X.-H.; Zuo, J.-L.; You, X.-Z. *Dalton Trans.* **2008**, 5593. (d) Mondal, K. C.; Mukherjee, P. S. *Inorg. Chem.* **2008**, *47*, 4215. (e) Jia, Q.-X.; Bonnet, M.-L.; Gao, E.-Q.; Robert, V. *Eur. J. Inorg. Chem.* **2009**, 3008. (f) Mukherjee, S.; Gole, B.; Chakrabarty, R.; Mukherjee, P. S. *Inorg. Chem.* **2009**, *48*, 11325. (g) Tian, C.-B.; Li, Z.-H.; Lin, J.-D.; Wu, S.-T.; Du, S.-W.; Lin, P. *Eur. J. Inorg. Chem.* **2010**, 427. (h) Sengupta, O.; Gole, B.; Mukherjee, S.; Mukherjee, P. S. *Dalton Trans.* **2010**, *39*, 7451. (i) Mukherjee, S.; Mukherjee, P. S. *Inorg. Chem.* **2010**, *49*, 10658.

(11) (a) Dutta, R. L.; Syamal, A. *Elements of Magnetochemistry*, 2nd ed.; East West Press: Manhattan Beach, CA, 1993. (b) Kahn, O. *Molecular Magnetism*; VCH Publishers: New York, 1993.

(12) *SMART/SAINT*; Bruker AXS, Inc.: Madison, WI, 2004.

(13) Sheldrick, G. M. *SHELX-97*; University of Göttingen: Göttingen, Germany, 1998.

(14) Farrugia, L. J. *J. Appl. Crystallogr.* **1999**, *32*, 837.Farrugia, L. J. *WinGX*, version 1.65.04; Department of Chemistry, University of Glasgow: Glasgow, Scotland, 2003.

(15) Sheldrick, G. M. *SADABS*; University of Göttingen: Göttingen, Germany, 1999.

(16) ORTEP-3 for Windows, version 1.08: Farrugia, L. J. *J. Appl. Crystallogr.* **1997**, *30*, 565.

(17) Ruiz, E.; Alemany, P.; Alvarez, S.; Cano, J. *J. Am. Chem. Soc.* **1997**, *119*, 1297.

(18) Ruiz, E.; Rodríguez-Fortea, A.; Cano, J.; Alvarez, S.; Alemany, P. *J. Comput. Chem.* **2003**, *24*, 982.

(19) Ruiz, E.; Cano, J.; Alvarez, S.; Alemany, P. *J. Comput. Chem.* **1999**, *20*, 1391.

(20) Ruiz, E. *Struct. Bonding (Berlin)* **2004**, *113*, 71.

(21) Becke, A. D. *J. Chem. Phys.* **1993**, *98*, 5648.

(22) Frisch, M. J.; Trucks, G. W.; Schlegel, H. B.; Scuseria, G. E.; Robb, M. A.; Cheeseman, J. R.; Montgomery, J. A.; Vreven, T.; Kudin, K. N.; Burant, J. C.; Millam, J. M.; Iyengar, S. S.; Tomasi, J.; Barone, V.; Mennucci, B.; Cossi, M.; Scalmani, G.; Rega, N.; Petersson, G. A.; Nakatsuji, H.; Hada, M.; Ehara, M.; Toyota, K.; Fukuda, R.; Hasegawa,

J.; Ishida, H.; Nakajima, T.; Honda, Y.; Kitao, O.; Nakai, H.; Klene, M.; Li, X.; Knox, J. E.; Hratchian, H. P.; Cross, J. B.; Adamo, C.; Jaramillo, J.; Gomperts, R.; Stratmann, R. E.; Yazyev, O.; Austin, A. J.; Cammi, R.; Pomelli, C.; Ochterski, J.; Ayala, P. Y.; Morokuma, K.; Voth, G. A.; Salvador, P.; Dannenberg, J. J.; Zakrzewski, V. G.; Dapprich, S.; Daniels, A. D.; Strain, M. C.; Farkas, O.; Malick, D. K.; Rabuck, A. D.; Raghavachari, K.; Foresman, J. B.; Ortiz, J. V.; Cui, Q.; Baboul, A. G.; Clifford, S.; Cioslowski, J.; Stefanov, B. B.; Liu, G.; Liashenko, A.; Piskorz, P.; Komaromi, I.; Martin, R. L.; Fox, D. J.; Keith, T.; Al-Laham, M. A.; Peng, C. Y.; Nanayakkara,A.; Challacombe, M.; Gill, P. M. W.; Johnson, B.; Chen, W.; Wong, M. W.; Gonzalez, C.; Pople, J. A. *Gaussian 03*, revision B.4; Gaussian Inc.: Pittsburgh, PA, 2003.

(23) Becke, A. D. *Phys. Rev. A* **1988**, *38*, 3098.

(24) Lee, C.; Yang, W.; Parr, R. G. *Phys. Rev. B* **1988**, *37*, 785.

(25) Ruiz, E.; Alvarez, S.; Cano, J.; Polo, V. *J. Chem. Phys.* **2005**, *123*, 164110.

(26) (a) Zajac, M. A.; Vedejs, E. *Org. Lett.* **2004**, *6*, 237. (b) Terada, M.; Toda, Y. *J. Am. Chem. Soc.* **2009**, *131*, 6354. (c) Terada, M.; Machioka, K.; Sorimachi, K. *Angew. Chem., Int. Ed.* **2009**, *48*, 2553.

(27) (a) Chen, X.; Rong, R.; Wang, Y.; Zhu, L.; Zhao, Q.; Ang, S. G.; Sun, B. *Eur. J. Inorg. Chem.* **2010**, 3506. (b) Liu, Z.-L.; Li, L.-C.; Liao, D.-Z.; Jiang, Z.-H.; Yan, S.-P. *Cryst. Growth Des.* **2005**, *5*, 783.